Quantum Dissipation in the Hydrodynamic Moment Hierarchy: A Semiclassical Truncation Strategy †

ARTICLE *in* THE JOURNAL OF PHYSICAL CHEMISTRY B · AUGUST 2002

Impact Factor: 3.3 · DOI: 10.1021/jp020845s

2 AUTHORS:

Jeremy B Maddox
Western Kentucky University
32 PUBLICATIONS **344** CITATIONS

SEE PROFILE

Eric R Bittner
University of Houston
128 PUBLICATIONS **2,033** CITATIONS

SEE PROFILE

Quantum Dissipation in the Hydrodynamic Moment Hierarchy: A Semiclassical Truncation Strategy†

Jeremy B. Maddox* and Eric R. Bittner‡

Department of Chemistry, University of Houston, Houston, Texas 77204

Received: March 29, 2002

In this paper we formulate the hydrodynamic moment and cumulant expansions of the density matrix for a quantum system in which the time evolution is described by an infinite hierarchy of coupled hydrodynamic moment equations. For the case where the system interacts with a complex environment, we develop a semiclassical closure that truncates the hierarchy. Our numerical approach for solving the truncated system of equations is intimately related to the de Broglie−Bohm interpretation of quantum mechanics, in that the time evolution of each cumulant is constructed over a discrete ensemble of hydrodynamic paths. We discuss the advantages and disadvantages of this scheme and apply the method to a model problem for a particle escaping from a metastable potential well while in contact with a thermal bath.

I. Introduction and Background

Classical molecular dynamics (MD) simulations play an integral role in understanding the dynamics of many systems of chemical and biological importance.[1,2] The primary assumption of MD is based upon the idea that the atoms in a molecular system follow well-behaved Newtonian trajectories. Despite its enormous popularity, the fundamental flaw with this description is that important quantum events such as tunneling and nonadiabatic transitions are inherently ignored in the dynamics. Because an explicit quantum mechanical treatment of both nuclear and electronic motion is not feasible for all but the simplest molecular systems, it is a practical necessity to partition the dynamics of a complex system into classical and quantum components. In light of the success with using classical atomic trajectories in MD, there has been a growing interest in the development of novel trajectory based methodologies for describing the dynamics of quantum systems. While such techniques may facilitate the use of interesting computational devices such as adaptive grids and time-dependent basis sets, the greatest motivation lies in finding systematic ways of partitioning between quantum and classical degrees of freedom in mixed quantum/classical simulations. Several recent contributions to this endeavor have involved hydrodynamic treatments,[3−6] semiclassical Liouville space representations,[7−10] semiclassical initial value representations,[11] and quantum-dressed classical dynamics.[12−15]

A. Hydrodynamic Representation of the Wave Function. The hydrodynamic approach is deeply rooted in the de Broglie−Bohm interpretation of quantum mechanics.[16−19] Here, one adopts the notion that the quantum wave function $\psi(x,t)$ acts as a driving field for an ensemble of hydrodynamic trajectories $\{x(t)\}$ that satisfy Newtonian-*like* equations of motion:

$$\dot{x}(t) = v(x(t),t) \tag{1}$$

According to the formulation, we write the wave function in polar form

$$\psi(x,t) = \exp\left(g(x,t) + \frac{i}{\hbar}S(x,t)\right) \tag{2}$$

where $g(x,t)$ is related to the logarithm of the quantum probability density and $S(x,t)$ is the quantum phase, or action. Typically, one associates a velocity field $v(x(t),t)$ with the gradient of the action along the set of hydrodynamic trajectories:

$$v(x(t),t) = \frac{1}{m}\partial_x S(x(t),t) \tag{3}$$

Substituting eqs 2 and 3 into the time-dependent Schrödinger equation, we readily obtain the time-dependence of $g(x,t)$

$$d_t g(x,t) = -\frac{1}{2}\partial_x v(x,t) \tag{4}$$

and $S(x, t)$

$$d_t S(x,t) = L(x,t) = \frac{1}{2}mv(x,t)^2 - V(x) + \frac{\hbar^2}{2m}(\partial_x{}^2 g(x,t) + (\partial_x g(x,t))^2) \tag{5}$$

where $L(x,t)$ is the quantum Lagrangian and $d_t = \partial_t + v(x,t)\partial_x$ is the total time derivative corresponding to the time rate of change in the reference frame of a fluid element moving along its trajectory $x(t)$. The last two terms on the right-hand side of eq 5 correspond to an effective potential consisting of both the classical external potential energy $V(x)$ and a quantum mechanical contribution aptly dubbed the "quantum potential". The quantum potential is often regarded as a strain energy associated with the curvature of the density field and is the source of nonlocal interactions between fluid particles. This leads to a type of ensemble force, similar to an osmotic pressure force, whereby particles are accelerated through and/or away from regions where the curvature of the density is very intense.[19] Because eqs 4 and 5 are completely isomorphic with the time-dependent Schrödinger equation, we can always decompose $\psi(x,t)$ into $g(x,t)$ and $S(x,t)$ in order compute a set of hydrody-

† Part of the special issue "John C. Tully Festschrift".

* Corresponding author. E-mail:jmaddox@uh.edu.

‡ E-mail: bittner@uh.edu.

10.1021/jp020845s CCC: $22.00
Published on Web 07/03/2002

namic trajectories. Alternatively, if we concoct a scheme for determining the solutions $g(x(t),t)$ and $S(x(t),t)$, then we can formally construct a pointwise representation of $\psi(x,t)$ over the ensemble of trajectories $\{x(t)\}$:

$$\psi(x(t),t) = \exp\left(-\frac{1}{2}\int_0^t \partial_x v(x(s),s)\, ds + \frac{i}{\hbar}\int_0^t L(x(s),s)\, ds\right)\psi(x(0),0) \quad (6)$$

where $L(x(t),t)$ is the quantum Lagrangian given by the right-hand side of eq 5. The fact that one can generally write a wave function in terms of an ensemble of hydrodynamic trajectories has led to the development of several computational methodologies for studying wave packet dynamics using techniques borrowed from computational fluid dynamics.[3,4]

B. Moving Least-Squares Method. The procedure we use here is based upon a moving weighted least-squares (MWLS) algorithm[20] as implemented in the quantum trajectory method (QTM) developed by Wyatt and co-workers for solving the time-dependent Schrödinger equation.[4,21] For simplicity we discuss only the one-dimensional case; however, the extension to multidimensional systems is fairly straightforward.[22] The basic workings of the method are as follows. The density, action, and velocity fields are discretized over an adaptive mesh of Lagrangian fluid elements. These particles are then collected into local neighborhoods, typically 5−15 points, over which a finite basis of simple polynomials $p_j(x) \in \{1, x, x^2/2, ..., x^{n_b}/n_b!\}$ provides a suitable representation for the fields. In each neighborhood, a given field $f(x)$ is expanded about the neighborhood's center of mass x_o so that the value of $f(x)$ at any other point x_i inside the neighborhood is given by

$$f(x_i)\, w(x_i - x_o) = \left(f(x_o) + \sum_j n_b a_j p_j(x_i - x_o)\right) w(x_i - x_o) \quad (7)$$

The Gaussian weighting function $w(x_i - x_o)$ scales the contribution of the surrounding neighbors such that points farther away from x_i have less impact in determining the expansion coefficients $\{a_j\}$ at x_i. Requiring that the number of neighbors exceeds the number of basis functions n_b ensures that we have an overdetermined set of least-squares equations, which are inverted to give the a_j's. Once the expansion coefficients are known, the local derivatives of $f(x)$ over the neighborhood of points are easily determined. The solutions $g(x(t),t)$, $S(x(t),t)$, and $x(t)$ are then propagated in time using a Verlet leapfrog method, where simple forward Eulerian integration is employed to advance the fields and trajectories over an atomic unit time-step.

The key feature of the MWLS scheme is that the mesh automatically adjusts to accommodate the expansion and contraction of the density's spatial extent. Because the grid evolves with the flow of density, we can effectively use fewer points in our calculations; however, this can also be problematic in the sense that the grid will rapidly become disorganized due to the presence of anharmonic terms in the classical and/or quantum potential fields. Left unchecked, this often leads to crossed trajectories, corresponding to a multivalued probability distribution, which is simply not allowed. To avoid the problem, we periodically reorganize the mesh back to a uniform grid and fit the pertinent fields onto the new mesh points using least-squares interpolation. This process is accurate provided that each new grid point is chosen to lie within the neighborhood of the corresponding original mesh point. Other methods for circumventing trajectory crossings have been implemented by Wyatt and Bittner in refs 23 and 24. Notwithstanding a few minor numerical complications, the hydrodynamic method has proven to be a useful alternative to traditional fixed-grid techniques and has been applied to a number of physical problems including photodissociation,[25] reactive scattering,[21] quantum tunneling effects,[6,24] nonadiabatic transitions,[22,26] and system/bath dynamics.[27−29] The classical-like feel of the dynamics and near linear scaling of computational overhead with the number of trajectories are among the primary motivations for the continued development of hydrodynamic based methodologies.

C. Hydrodynamic Representation of the Density Matrix. Recently, we extended the de Broglie−Bohm formalism to accommodate a Liouville-space representation of a quantum state by constructing the density matrix $\rho(x,y) = \psi(x)\, \psi^*(y)$ over a 2-D ensemble of Lagrangian fluid elements.[28−31] For this we find it convenient to express the density matrix in terms of the relative variables $q = (x + y)/2$ and $z = x - y$. In this rotated coordinate frame we write the density matrix in polar form

$$\rho(q,z,t) = \exp\left(g(q,z,t) + \frac{i}{\hbar}S(q,z,t)\right) \quad (8)$$

where $g(q,z)$ is now the logarithmic amplitude of $\rho(q,z)$ and $S(q,z)$ is the effective action in Liouville space. By "effective" we mean that $S(q,z)$ is the phase difference between the forward-time evolution of $\psi(x)$ and the reverse-time evolution of $\psi^*(y)$. The time evolution of $\rho(q,z)$ is given by the Liouville−von Neumann equation

$$i\hbar\dot{\hat{\rho}} = [\hat{H},\hat{\rho}] \quad (9)$$

Writing eq 9 in terms of q and z, we have

$$i\hbar\partial_t\rho(q,z,t) = -\frac{\hbar^2}{m}\partial_{qz}{}^2\rho(q,z,t) + \tilde{V}(q,z)\, \rho(q,z,t) \quad (10)$$

where $\tilde{V}(q,z) = V(q+z/2) - V(q-z/2)$ is the effective classical potential energy surface. We represent $\rho(q,z,t)$ over an ensemble of hydrodynamic trajectories that obey the following equations of motion:

$$\dot{q}(t) = v_q(q,z,t) = \partial_z S(q,z,t)/m \quad (11)$$

$$\dot{z}(t) = v_z(q,z,t) = \partial_q S(q,z,t)/m \quad (12)$$

where this relationship between the velocity field components and the effective action is again due to the fact that $\rho(x,y)$ has both forward and backward propagating components. Following the procedure outlined in section I(A), we substitute eq 8 into eq 10 and formulate analogous equations of motion for $g(q,z,t)$

$$d_t g(q,z) = -\frac{1}{m}\partial_{qz}{}^2 S(q,z) = -\partial_q\dot{q} \quad (13)$$

and $S(q,z)$

$$d_t S(q,z) = m\dot{q}\dot{z} - \tilde{V}(q,z) - \tilde{Q}(q,z) \quad (14)$$

where

$$\tilde{Q}(q,z) = Q(q + z/2) - Q(q - z/2) = -\frac{\hbar^2}{m}(\partial_{qz}{}^2 g(q,z) + \partial_q g(q,z)\, \partial_z g(q,z)) \quad (15)$$

is the effective quantum potential. Given the solutions of eqs

11−14, we can always construct a pointwise representation of $\rho(q,z,t)$ over a discrete ensemble of hydrodynamic trajectories $\{q(t), z(t)\}$:

$$\rho(q(t),z(t),t) = \exp\left(-\int_0^t \partial_q \dot{q}(s)\, ds + \frac{i}{\hbar}\int_0^t \mathcal{L}(q(s),z(s),s)\, ds\right)\rho(q(0),z(0),0) \quad (16)$$

where $\mathcal{L}(q(t),z(t),t)$ is the effective Lagrangian related to the total time derivative $S(q,z,t)$ along the set paths parametrized by t. We have applied the MWLS method to eq 16 for a number of model problems involving both dissipative and nondissipative dynamics.[28,29] In the former case, where a quantum system is in contact with a complex thermal environment, we have illustrated the novelty of hydrodynamic trajectories as a computational tool for probing dissipative effects such as decoherence and energy relaxation. Our analysis concerns two types of hydrodynamic trajectories corresponding to the evolution of the diagonal ($z = 0$) and off-diagonal ($z \neq 0$) elements of the reduced density matrix. Dissipation causes the diagonal trajectories to relax to some stationary configuration, reflecting upon the thermal populations of the equilibrium state. The off-diagonal trajectories are accelerated toward $z \rightarrow \pm\infty$ corresponding to the continuous entanglement between the system and bath degrees of freedom. As the off-diagonal trajectories stream away from the diagonal axis, the amplitude they carry is exponentially damped by decoherence, which tends to force $\rho(q,z)$ into a sharply localized Gaussian about $z = 0$. This effect is counterbalanced by the quantum force that acts to minimize the strain energy associated with the curvature of the density, ultimately resulting in an equilibrium between decoherence and the outward pressure of the quantum force. Moreover, for high-temperatures this equilibrium is established on a time scale much smaller than the typical time for energy relaxation. Consequently, we are led to hypothesize that there may be some benefit to formulating a truncated description of the dynamics along z.

In this paper we formulate the hydrodynamic moment and cumulant expansions of the density matrix.[30−35] This is quite different from the previous situation where we have treated both q and z explicitly. Here, the z dependence of $\rho(q,z)$ is developed through an infinite series of moments and cumulants defined over a set fluid elements evolving along q only. From the master equation governing the time evolution of $\rho(q,z)$ we derive an infinite hierarchy of coupled equations that relate the evolution of the hydrodynamic moments and cumulants to the ensemble of fluid trajectories. The central problem of this approach involves truncating the hierarchy while at the same time retaining convergence in the series expansion of $\rho(q,z)$. For open systems, we show that dissipative effects allow us to approximately close the hierarchy at second order in the cumulants. We discuss the physical insight gained in the hydrodynamic moment representation and explore an alternative expansion scheme based upon Gauss−Hermite polynomials. We discuss the computational benefits and caveats of incorporating the cumulant expansion into a numerical scheme and apply this approach to a model problem for a particle escaping from a metastable potential well.

II. Theoretical Overview

A. Wigner Function. In the search for a classical-*like* description of a quantum system, we exploit the procedure outlined by Wigner,[36] whereby one finds quantum mechanical corrections to the classical Liouville equation by relating the quantum density matrix to a *pseudo*probability distribution function defined in a phase space where p is the canonical momentum of the coordinate q. Taking a Fourier transform of $\rho(q,z)$ with respect to z and p, we have

$$W(q,p) = \frac{1}{2\pi\hbar}\int_{-\infty}^{\infty}\rho(q,z)e^{-ipz/\hbar}\, dz \quad (17)$$

where we note that the Wigner function $W(q,p)$ is an exact representation, equivalent to $\rho(q,z)$. One particularly useful feature of $W(q,p)$ is its relationship to the distribution functions encountered in the hydrodynamic analogy of quantum mechanics. Specifically, we can write

$$\rho(q) = \int_{-\infty}^{\infty}(q,p)\, dp \quad (18)$$

$$j(q) = \frac{1}{m}\int_{-\infty}^{\infty} pW(q,p)\, dp \quad (19)$$

$$T(q) = \frac{1}{2m}\int_{-\infty}^{\infty} p^2 W(q,p)\, dp \quad (20)$$

for the probability density, probability current density, and kinetic energy density, respectively. Taking the Fourier transform of eq 10 and assuming that $\tilde{V}(q,z)$ can be expanded in a Taylor series about $z = 0$, we obtain the time dependence of $W(q,p)$

$$\partial_t W(q,p) = -\frac{p}{m}\partial_q W(q,p) + \sum_{k=0}^{\infty}\left(\frac{\hbar}{2i}\right)^{2k}\frac{1}{(2k+1)!}\partial_q{}^{2k+1}V(q)\partial_p{}^{2k+1}W(q,p) \quad (21)$$

Indeed, it is easy to show that as $\hbar \rightarrow 0$, eq 21 reduces to the classical Liouville equation; thus Wigner's analysis provides a natural extension of classical mechanics via the addition of quantum mechanical corrections with increasing order in $\hbar$.

It is often noted that the Wigner function cannot be regarded as a true probability density due to the fact that $W(q,p)$ becomes negative in certain regions of phase space when there are long-range isolated coherences in the density matrix. For the case of a particle subjected to the influence of a complex environment (e.g., a massive Brownian particle submersed in thermal bath), it is known that thermal fluctuations in the surrounding medium, acting as weak measurements, tend to dampen the phase correlations between position eigenstates. At high enough temperatures decoherence will ultimately diagonalize the density matrix. The corresponding Wigner function then becomes completely positive, resembling a true phase space distribution, and the quantum particle is expected to exhibit more or less classical behavior.

B. Classical Limits of Quantum Dissipation. The dynamics of a classical particle in contact with a heat bath are well understood and typically described by the Langevin equation,

$$m\ddot{q} + \eta\dot{q} + V'(q) = F(t) \quad (22)$$

where η is a damping constant and $F(t)$ is a random force representing the collective influence of the surrounding environment on the particle. Assuming the environment retains no memory of its previous interaction with the system, the fluctuating force will obey Gaussian statistics

$$\langle F(t)\rangle = 0$$
$$\langle F(t)\,F(0)\rangle = 2\eta kT\delta(t) \quad (23)$$

If we consider the distribution of all possible trajectories in phase space $P(q,p,t)$, we are led to the Chandrasekhar equation[37]

$$\partial_t P(q,p,t) = -\frac{p}{m}\partial_q P(q,p,t) + V'(q)\partial_p P(q,p,t) + 2\gamma\partial_p(pP(q,p,t)) + 2m\gamma kT\partial_p{}^2 P(q,p,t) \quad (24)$$

where $\gamma = \eta/2m$ is a relaxation constant. Because we cannot write a set of Hamilton or Lagrange equations describing the motion a particle subjected to a stochastic force, the standard procedures of quantization are not applicable. Rigorous correspondence calls for the explicit treatment of both the particle and bath dynamics. Typically, in condensed phase chemical physics, this involves an astronomical number of degrees of freedom. Clearly we must find a way to reduce the dimensionality of the problem without sacrificing the dynamics. The literature pertaining to this subject is quite vast and there are a wide variety of theoretical models to choose from.[38] The Feynman−Vernon influence functional approach[39] is one popular technique that has been used to derive several master equations describing the evolution of a quantum system in contact with a thermal bath. The simplest of these, due to Caldeira and Leggett,[40] was originally formulated to describe the classical limits of quantum Brownian motion. In operator form the Caldeira−Leggett (CL) master equation is given by

$$i\hbar\partial_t\rho = [H,\rho] + \gamma\left([x,\rho p] - [p,\rho x] + \frac{1}{2}[\{p,x\},\rho]\right) - \frac{i\hbar}{\Lambda^2}[x,[x,\rho]] \quad (25)$$

where H is the Hamiltonian for the isolated particle, $\Lambda = \hbar/\sqrt{2mkT}$ is the thermal de Broglie wavelength, and [,] and {,} stand for the commutator and anticommutator. We can see that the bath's influence supplements the ordinary Liouville−von Neumann equation with the addition of several dissipative terms. Writing the dissipative parts of eq 25 in terms of q and z gives

$$\partial_t\rho_{\mathrm{diss}}(q,z) = -2\gamma\partial_z\rho(q,z) - \frac{\gamma z^2}{\Lambda^2}\rho(q,z) \quad (26)$$

where the first term on the right-hand side, corresponding to friction, facilitates the dissipative coupling between the system and its environment. Here, the phenomenological dissipation constant γ sets the time scale for the relaxation of kinetic energy

$$\tau_{\mathrm{R}} = \gamma^{-1} \quad (27)$$

Decoherence is induced by the second term on the right in eq 26 where Λ contributes a temperature dependence to lifetime of a coherence between two position eigenstates separated by a distance $|z|$:

$$\tau_{\mathrm{D}} = \gamma^{-1}\Lambda^2/z^2 \quad (28)$$

Taking the Fourier transform of eq 26 with respect to z and p, we can develop the corresponding pair of dissipative terms for the Wigner function

$$\partial_t W_{\mathrm{diss}}(q,p) = 2\gamma\partial_p(pW(q,p)) + 2m\gamma kT\partial_p{}^2 W(q,p) \quad (29)$$

which are identical to the classical dissipation terms in eq 24. It is worth mentioning that eq 25 is not completely adequate as it does not preserve the positivity of $\hat{\rho}$ and is only valid in the high-temperature regime where kT is much greater than the zero-point energy of the uncoupled system. Other master equations have been formulated to explicitly include low-temperature effects such as zero-point motion[41] and colored noise.[42,43] However, these treatments lead to the presence of time-dependent coefficients in the friction and decoherence terms and would be quite challenging to implement numerically.

In what follows we shall develop a hierarchy of moment equations for the reduced density matrix that are related to the hydrodynamic distributions in eqs 18−20. Our strategy is to represent the quantum density matrix in terms of these moments, which we define over an ensemble of hydrodynamic trajectories. We then argue that the dissipative terms in eq 26 and 29 allow us to approximately close the infinite hierarchy of equations leading to a novel semiclassical methodology for modeling the dynamics of dissipative systems.

III. Cumulant Representation

Starting with a Taylor series expansion of $\rho(q,z)$ about $z = 0$ and utilizing the inverse Fourier relation of eq 17, we write the density matrix as a series of momentum integrals:[30−35]

$$\rho(q,z) = \sum_{n=0}^{\infty}\frac{z^n}{n!}\frac{\partial^n\rho}{\partial z^n}\Big|_{z=0} = \sum_{n=0}^{\infty}\frac{z^n}{n!}\int_{-\infty}^{\infty}\left(\frac{ip}{\hbar}\right)^n W(q,p)\,\mathrm{d}p = \sum_{n=0}^{\infty}\left(\frac{iz}{\hbar}\right)^n\frac{\rho_n(q)}{n!}. \quad (30)$$

For simplicity, we shall refer to ρ_n as the nth moment of the Wigner function. Following the method of moments[44] it is straightforward to develop an infinite hierarchy of equations for the time evolution of the ρ_n's. Adding eqs 21 and 29, we multiply by p^n and integrate over p to obtain

$$\partial_t\rho_n = -\frac{1}{m}\partial_q\rho_{n+1} - \sum_{k=0}^{(n-1)/2}\left(\frac{\hbar}{2i}\right)^{2k}\binom{n}{2k+1}\partial_q{}^{2k+1}V\rho_{n-2k-1} - 2n\gamma\rho_n + 2m\gamma kT\rho_{n-2} \quad (31)$$

where $\binom{n}{m}$ is the binomial coefficient. The first few moments of the hierarchy carry the usual physical interpretation. In the context of hydrodynamic quantities, ρ_0 is easily identified with a probability density and satisfies the continuity equation $\partial_t\rho_0 = -\partial_q\rho_1/m$. Likewise, ρ_1/m and $\rho_2/2m$ are interpreted as a probability current density and kinetic energy density, respectively. Despite the fact that these terms have a natural physical interpretation, the Taylor series expansion of $\rho(q,z)$ is expected to converge very slowly (even for a simple Gaussian) and is not well-suited for numerical implementation. Faced with this, we invoke a cumulant expansion of $\rho(q,z)$ about $z = 0$. Using eq 8, we recast the moment expansion in a form amenable to the de Broglie−Bohm interpretation of quantum mechanics:[30,31,45]

$$\rho(q,z) = \exp\left[\sum_{n=0}^{\infty}\frac{z^n}{n!}\left(g^{(n)}(q) + \frac{i}{\hbar}S^{(n)}(q)\right)\right] \quad (32)$$

where the cumulants are given by $g^{(n)} = \partial_z^n g(q,z)|_{z=0}$ and $S^{(n)} = \partial_z^n S(q,z)|_{z=0}$ and the Hermiticity of $\hat{\rho}$ requires that $g^{(n)} = 0$ and $S^{(n)} = 0$ for odd and even n, respectively. Substituting eq 8 into eq 30 and equating term by term with eq 31, we generate the cumulant equations of motion:

$$\partial_t g^{(0)} = -\frac{1}{m}(\partial_q S^{(1)} + S^{(1)}\partial_q g^{(0)})$$

$$\partial_t S^{(1)} = -V' + \frac{\hbar^2}{m}(\partial_q g^{(2)} + g^{(2)}\partial_q g^{(0)}) - \frac{1}{m}S^{(1)}\partial_q S^{(1)} - 2\gamma S^{(1)}$$

$$\partial_t g^{(2)} = -\frac{1}{m}(\partial_q S^{(3)} + 2g^{(2)}\partial_q S^{(1)} + S^{(3)}\partial_q g^{(0)}) - \frac{1}{m}S^{(1)}\partial_q g^{(2)} - 2\gamma g^{(2)} - \frac{4m\gamma kT}{\hbar^2}$$

$$\vdots$$

$$\partial_t Q^{(n>2)}_{\text{even } n} = -2n\gamma Q^{(n)} - \frac{1}{m}\partial_q Q^{(n+1)} - \frac{1}{m}\sum_{k=0}^{n}\binom{n}{k}Q^{(n-k+1)}\partial_q Q^{(k)}$$

$$\partial_t Q^{(n)}_{\text{odd } n} = -2n\gamma Q^{(n)} - \frac{V^{(n)}}{2^{n-1}} + \frac{\hbar^2}{m}\partial_q Q^{(n+1)} + \frac{\hbar}{m}\sum_{k=0}^{n}(-1)^k\hbar^{(-1)^k}\binom{n}{k}Q^{(n-k+1)}\partial_q Q^{(k)} \quad (33)$$

where we have used a generalized cumulant $Q^{(n)}$ to represent both $g^{(n)}$ and $S^{(n)}$ for even and odd n, respectively.

Let us first consider the case of the uncoupled system (i.e., $\gamma = 0$). The structure of the hierarchy outlined in eq 33 is obviously complicated by the fact that the equation of motion for each member contains both higher and lower order terms. Consequently, there is no general way to exactly close the system of equations. We can attempt an approximate closure by setting one of the higher order odd moments to zero. At first glance this procedure seems reasonable because the $1/n!$ coefficient in eq 32 depresses the contribution of the higher order cumulants to the density matrix. However, as the cumulants evolve, the error introduced in the equations of motion by neglecting such a term will eventually creep down and back up the hierarchy, leading to larger errors at later times. This effect is illustrated in Figure 1 for an undamped squeezed state in a harmonic well. The set of curves correspond to the first five cumulants of $\rho(q,z)$ and we have ignored fifth-order and higher terms in the dynamics. For the first 2000 time steps there does not appear to be anything out of the ordinary. At $t = 2440$ au we can see that $S^{(3)}$ and $g^{(4)}$ have accumulated a small amount of error at the ends of the grid and by $t = 2700$ au the error has propagated into $g^{(2)}$ and $S^{(1)}$. By $t = 2900$ au the errors have dramatically snowballed and the calculation soon falls apart. As it turns out, we can reconcile this situation by reinstating the dissipative terms in eq 33. Notice that the damping terms increase in magnitude with the order of the cumulants. At some point we would expect damping to dominate over the errors introduced by neglecting a higher order cumulant, therefore making it feasible to approximately close the hierarchy. Figure 2 shows the cumulants for the same state as in Figure 1; however we have included the effects of dissipation. The dissipative terms in eq 33 stabilize the dynamics and the truncated system of cumulants quickly relaxes to equilibrium without suffering any numerical problems.

It is interesting to note that thermal effects are introduced solely in the $g^{(2)}$ cumulant and that the other members of the

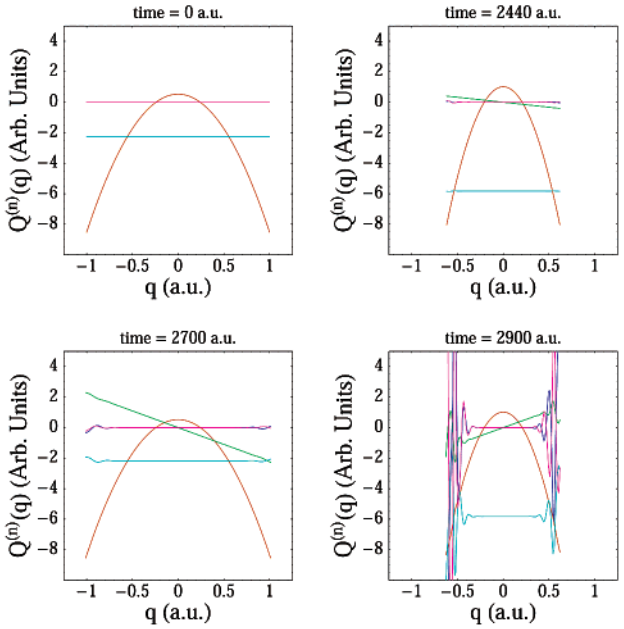

Figure 1. Time evolution of the first five density cumulants for an undamped particle $m = 2000$ au in a harmonic oscillator potential with frequency $\hbar\omega/k = 2232$ K and period $\tau = 888$ au. The dashing convention for the cumulants is as follows: (orange) $g^{(0)}$, (green) $S^{(1)}$, (light blue) $g^{(2)}$, (dark blue) $S^{(3)}$, (purple) $g^{(4)}$ and we have ignored the fifth order and higher terms in the equations of motion. The accumulation of error in the cumulants is clearly visible after just a few oscillation periods.

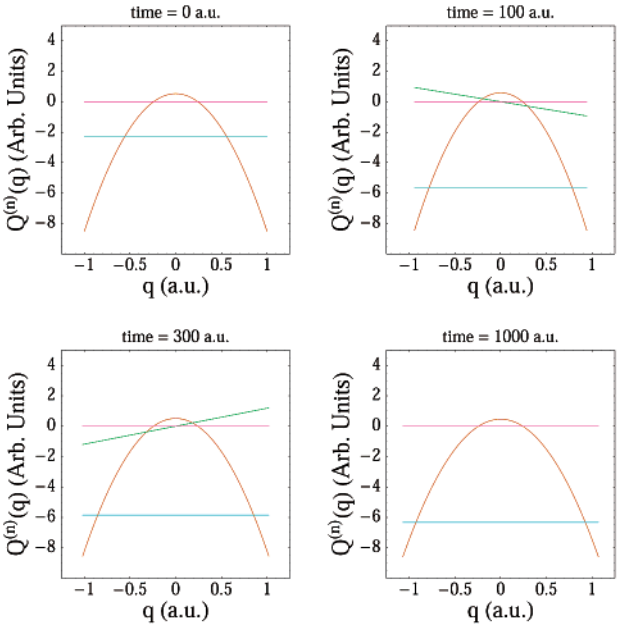

Figure 2. Same scenario as in Figure 1 only the effects of a heat bath have been included. For the underdamped oscillator $\gamma = 0.75\omega$ at $T = 2000$ K the cumulants quickly relax before any significant errors can build-up. Though it is not illustrated the configuration of the cumulants at time $t = 1000$ au is stable for many more oscillation periods.

hierarchy are only indirectly affected by temperature through the multitude of cross terms. While this may seem rather odd at first, it makes sense when we ascribe physical meaning to the cumulants. We write the probability density in terms of the zeroth-order cumulant

$$\rho(q(t),t) = \exp(g^{(0)}(q(t),t)) \quad (34)$$

which is now defined pointwise over the ensemble of hydro-

dynamic trajectories $\{q(t)\}$, satisfying $\dot{q}(t) = p(q(t),t)/m$. The probability current density is related to the first-order momentum cumulant $j(q) = S^{(1)}\rho_0/m$, and we can easily identify $S^{(1)}$ as a momentum field:

$$p(q(t),t) = S^{(1)}(q(t),t) \tag{35}$$

According to eq 33, the evolution of the momentum field is determined by both a classical force and a quantum force

$$F_Q = \frac{\hbar^2}{m}(\partial_q g^{(2)} + g^{(2)}\partial_q g^{(0)}) \tag{36}$$

Writing $g^{(2)}$ in terms of the original hydrodynamic moments

$$g^{(2)}(q) = -\frac{1}{\hbar^2}\left(\frac{\rho_2(q)}{\rho_0(q)} - \left(\frac{\rho_1(q)}{\rho_0(q)}\right)^2\right) \tag{37}$$

we see that it is related to the fluctuations in the kinetic energy distribution of the particle. In this way it becomes clear that the thermal term in the $g^{(2)}$ cumulant of eq 33 corresponds to the bath's contribution to the fluctuations in the particle's kinetic energy density.

It is worthwhile to point out that eq 36 is not unique to quantum mechanics. We can see that by substituting eq 37 into eq 36 the resulting expression

$$F_Q = \frac{1}{m}\left(-\left(\frac{\rho_1}{\rho_0}\right)^2\frac{\partial_q\rho_0}{\rho_0} + 2\frac{\rho_1}{\rho_0}\frac{\partial_q\rho_1}{\rho_0} - \frac{\partial_q\rho_2}{\rho_0}\right) \tag{38}$$

does not explicitly contain $\hbar$. Moreover, it is not difficult to show that this force is also present in the moment expansion of the classical Liouville equation. Using the definitions

$$\rho_0(q) = \rho(q) \tag{39}$$

$$\rho_1(q) = p(q)\,\rho(q) = mj(q) \tag{40}$$

$$\rho_2(q) = p(q)^2\,\rho(q) - \frac{\hbar^2}{4}\rho(q)\partial_q{}^2 \log \rho(q) = 2mT(q) \tag{41}$$

we can recover either the standard Bohmian expression for the quantum force in terms of $\rho(q)$ alone,

$$F_Q = -\partial_q\left(-\frac{\hbar^2\,\partial_q{}^2\rho(q)^{1/2}}{2m\;\;\rho(q)^{1/2}}\right) \tag{42}$$

or equivalently,

$$F_Q = -m\left(\frac{j(q)}{\rho(q)}\right)^2\frac{\partial_q\rho(q)}{\rho(q)} + 2m\frac{j(q)}{\rho(q)}\frac{\partial_q j(q)}{\rho(q)} - 2\frac{\partial_q T(q)}{\rho(q)} \tag{43}$$

This suggests that the quantum force has a classical analogue in the context of ensemble dynamics and that its form is determined by the statistical nature of the particle's description independently of whether the particle is classified as classical or quantum mechanical. The truly quantum components of the dynamics enter the moment hierarchy through the coupling terms that involve the density moments and higher odd order derivatives of the potential energy surface.

If we assume that decoherence occurs over an infinitesimally short time scale then the damping and thermal terms will dominate the evolution of $g^{(2)}$ and we can approximately close eq 33 by ignoring $S^{(3)}$ and higher order cumulants. Following this through, the truncated equations of motion for the cumulants are given by

$$d_t g^{(0)}(q) = -\frac{1}{m}\partial_q p(q,t)$$

$$d_t p(q) = -V' + \frac{\hbar^2}{m}(\partial_q g^{(2)}(q,t) + g^{(2)}(q,t)\partial_q g^{(0)}(q,t)) - 2\gamma p(q,t)$$

$$d_t g^{(2)}(q) = -\frac{2}{m}g^{(2)}(q,t)\partial_q p(q,t) - 2\gamma g^{(2)}(q,t) - 2\gamma\Lambda^2 \tag{44}$$

where $d_t = \partial_t + p\partial_q/m$ is the Lagrangian time derivative. The solutions of eq 44 allow us to construct the density matrix over the ensemble of trajectories as follows:

$$\rho(q(t),z,t) = \exp\left(g^{(0)}(q(t),t) + \frac{\mathrm{i}}{\hbar}S^{(1)}(q(t),t)z + g^{(2)}(q(t),t)\frac{z^2}{2}\right) \tag{45}$$

where have made the approximation that $\rho(q,z)$ is strictly Gaussian along z. For comparison sake, let us consider the explicit representation of $\rho(q,z)$. As discussed earlier, we can construct $\rho(q,z)$ by fitting the fields $g(q,z)$ and $S(q,z)$ using the MWLS method. Typically in our numerical implementation, we employ 21 grid points in each dimension and the equations of motion require us to evaluate both first- and second-order spatial derivatives over the full grid in q and z. For the truncated cumulant expansion approach we again use the MWLS algorithm and generally 101 points (but as few as 51 points) along only q. Computationally it is easier and more accurate to implement the cumulant representation in the sense that there are only first-order derivatives in the equations of motion. Because fewer trajectories are required to propagate the cumulants in time, the computational overhead is significantly less when compared to the full grid representation. Another useful feature of the cumulant expansion is that we can very easily switch back and forth between moving and stationary hydrodynamic representations (i.e., Lagrangian vs Eulerian reference frames) by simply changing the upper limit on the sums in eq 33 from n to $n - 1$. This suggests the possibility of developing hybrid methodologies by mixing adaptive techniques with traditional basis sets.

Unfortunately there are no free rides here and we have to pay a price for these computational benefits. Because eq 45 contains at most second-order cumulants, we automatically forfeit the ability to model intricate superposition states. While simply including more cumulant terms does allow for more interesting structures in $\rho(q,z)$, there is a diminishing return associated with the number of cumulants required to obtain good convergence in eq 32. From a semiclassical point of view though, this approximation is justified because as the quantum system is subjected to greater thermal energies it is less likely that coherences in $\rho(q,z)$ will survive beyond a very short time scale. On the other hand, if we wish to probe the short-time effects of dissipation, then we must either find a more versatile moment representation or revert back to explicitly treating the dynamics of $\rho(q,z)$ along z. Faced with this we explore an alternative expansion of the Wigner function based upon orthogonal polynomials.

IV. Gauss−Hermite Moment Representation

An alternative to the cumulant expansion of $\rho(q,z)$ is to expand the Wigner function as a series of orthogonal polynomials. We have elected to use the Gauss−Hermite polynomials

to explore this and in doing so, we write the Wigner function as

$$W(q,p) = \sum_{n=0}^{\infty} a_n(q)\, H_n(p/\sqrt{2}\sigma_p) \tag{46}$$

where $H_n(u)$ is the nth-order Hermite polynomial and σ_p is an arbitrary scaling parameter that keeps proper units and allows us to adjust the radius of convergence for the series. By orthogonality the expansion coefficients $a_n(q)$ are given by

$$a_n(q) = \frac{1}{2^n n!(2\pi\sigma_p^{\,2})^{1/2}} \int_{-\infty}^{\infty} H_n(p/\sqrt{2}\sigma_p) \times \exp(-p^2/2\sigma_p^{\,2}) W(q,p)\, \mathrm{d}p$$

$$= \frac{h_n(q)}{2^n n!(2\pi\sigma_p^{\,2})^{1/2}} \tag{47}$$

and for simplicity we shall refer to the integral represented by $h_n(q)$ as the nth Gauss−Hermite moment of $W(q,p)$. It is somewhat interesting to note that these coefficients can be related to the Husimi distribution function given by the convolution of $W(q,p)$ with a coherent state:[46]

$$W_{\mathrm{H}}(q,p) = \frac{1}{\pi\hbar} \int\int \exp\left(-\frac{(q'-q)^2}{2\sigma_q^{\,2}} - \frac{(p'-p)^2}{2\sigma_p^{\,2}} \right) \times W(q',p')\, \mathrm{d}q'\, \mathrm{d}p' \tag{48}$$

Using the generating function for the Hermite polynomials

$$\exp(2xt - t^2) = \sum_{n}^{\infty} \frac{H(x)t^2}{n!} \tag{49}$$

we can rewrite the momentum integral in eq 48 in terms of the Gauss−Hermite moments

$$W_{\mathrm{H}}(q,p) = \frac{1}{\pi\hbar} \sum_{n=0}^{\infty} \frac{1}{n!} \left(\frac{p}{\sqrt{2}\sigma_p} \right)^n \int \exp\left(-\frac{(q'-q)^2}{2\sigma_q} \right) h_n(q')\, \mathrm{d}q' \tag{50}$$

In this way, the Gauss−Hermite expansion resembles a partial Husimi transformation over momentum only. As before, we can use the method of moments to find a hierarchy of equations of motion for the Gauss−Hermite moments:

$$\partial_t h_n = -\frac{1}{2m\sigma_p} \partial_q (h_{n+1} + 2n h_{n-1}) + \frac{\sigma_p}{2} \sum_{k=0}^{\infty} \left(\frac{\hbar\sigma_p}{4\mathrm{i}} \right)^{2k} \frac{\partial_{\mathrm{q}}^{\,2k+1} V}{(2k+1)!} h_{n+2k+1} + \frac{\gamma}{2} \left(1 + \frac{\sigma_p^{\,2} m\gamma kT}{2} \right) h_{n+2} + \gamma(n+1) h_n \tag{51}$$

This hierarchy of equations is a bit more complicated than eq 31, in that the sum in eq 51 can only be truncated when the potential energy surface has a finite number of derivatives or when a local harmonic approximation of the potential surface is warranted.

In Figure 3 we qualitatively explore the convergence of the Gauss−Hermite moment expansion for two test cases. First we consider a superposition of two displaced Gaussian wave packets. The Wigner function for this state is given by

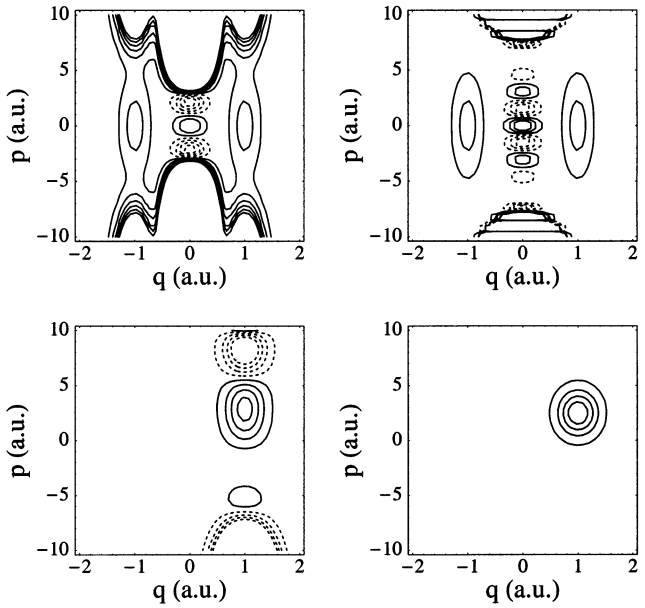

Figure 3. Qualitative illustration of convergence for the Gauss-Hermite moment expansion of the Wigner function. The upper left and right panels respectively correspond to a 6 and 30 term moment expansion for the superposition of two displaced Gaussian wave packets. Solid and dashed contours represent positive and negative values of $W(q, p)$, respectively. The lower left and right panels illustrate the 6 and 30 term expansion for a coherent state with nonzero average position and momentum.

$$W(q,p) = N \exp\left(-\frac{q^2}{\sigma_q^{\,2}} - \frac{p^2\sigma_q^{\,2}}{\hbar^2} \right) \left(\cos\left(\frac{2ap}{\hbar} \right) + \cosh\left(\frac{2aq}{\sigma_q^{\,2}} \right) \mathrm{e}^{-a^2/\sigma_q^{\,2}} \right) \tag{52}$$

where $2a$ is the distance between the Gaussian peaks, $\sigma_q^{\,2}$ is the variance along q for the individual Gaussians, and N is an unimportant normalization factor. The upper left- and right-hand panels of Figure 3 show the Gauss−Hermite moment expansion of $W(q,p)$ with six and thirty moments, respectively. We see that while the six term expansion displays all the important features of eq 52, it does not represent the state nearly as well as the thirty term moment expansion. The lower panels of Figure 3 illustrate the convergence of the Gauss−Hermite expansion for a coherent state having nonzero average position and momentum in phase space. The coherence state is easily represented by the cumulant expansion with only three terms. The convergence of the Gauss−Hermite expansion for a state with nonzero average momentum is diminished due to the fact that the Gauss−Hermite polynomials are centered about $p = 0$. The lower left- and right-hand panels again correspond to a six and thirty term expansion of $W(q,p)$, respectively. We see that there is a significant buildup of oscillations in the six term case, which are smoothed out by including a larger number of moments in the expansion. Dissipation will be very helpful in this situation because the average momentum of $W(q,p)$ will relax to zero over some finite time period. For the undamped case we note that the convergence of the expansion would be enhanced by computing the moments about the average momentum rather than $p = 0$.[33,34] Though we have not yet implemented the Gauss−Hermite moment expansion into a computational methodology its worthwhile to briefly explore

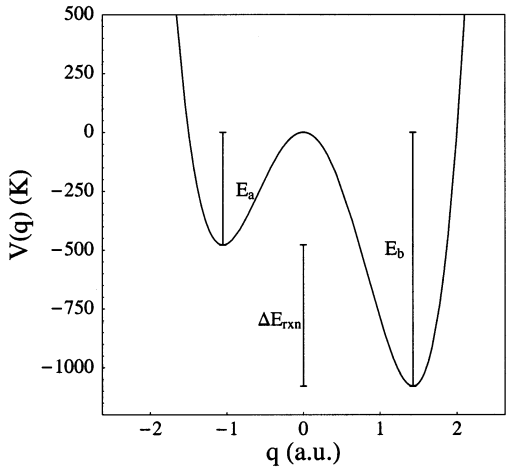

Figure 4. Potential energy curve for a model chemical reaction. The activation energy E_a for a reactant initially confined in the meta-stable well is 477 K and the energy difference between the reactants and products ΔE_{rxn} is roughly 600 K.

the possibility. We must find an appropriate finite representation for evaluating the spatial derivatives in eq 51. Since the Gauss−Hermite moments are expected to be highly oscillatory compared to the cumulants, it is likely that fitting via the MWLS procedure will be very difficult. One obvious choice would be to invoke a discrete variable representation (DVR) involving Gauss−Hermite basis functions.[47] Using techniques similar in spirit to Billing's quantum-dressed classical methods,[12] one could employ time-dependent Gauss−Hermite DVR's in order to efficiently converge the Gauss−Hermite moment expansion using a minimum number of terms.

V. Model Chemical Reaction

Consider a particle with mass $m = 2000$ au, escaping from the metastable potential well illustrated in Figure 4. The potential surface for this system is defined by

$$V(q) = \alpha q^4 + \beta q^3 + \delta q^2 \tag{53}$$

where $\alpha = 0.001$ au, $\beta = -0.0005$ au, and $\delta = -0.003$ au. Initially, the particle is represented by a Gaussian wave packet centered about the left-hand well. We compare the reaction probability as a function of time and temperature for three cases. In the first case the coherence length is set by the thermal de Broglie wavelength $\Lambda = \hbar/\sqrt{2mkT}$, as dictated by the CL model. The density matrix is constructed by numerically solving the set of truncated semiclassical equations of motion in eq 44. This is accomplished by using the MWLS method to propagate the cumulants over an ensemble of hydrodynamic trajectories. Figures 5 and 6 illustrate the evolution of $\exp(g(q,z))$ where the relationship between decoherence and temperature is immediately visible. At $T = 500$ K the width of the density packet along z remains virtually unchanged while at $T = 1200$ K the width is noticeably narrowed. Moreover, there is no buildup of coherence and the density matrix retains a Gaussian form along z throughout its evolution, thus signifying that the flux of density across the potential barrier occurs via thermal excitations rather than tunneling.

For the second case we replace Λ with an ad hoc coherence length λ_c computed from the thermal equilibrium density matrix $\hat{\rho}_{eq}$. For a system described by the Hamiltonian $\hat{H}$, $\hat{\rho}_{eq}$ is given

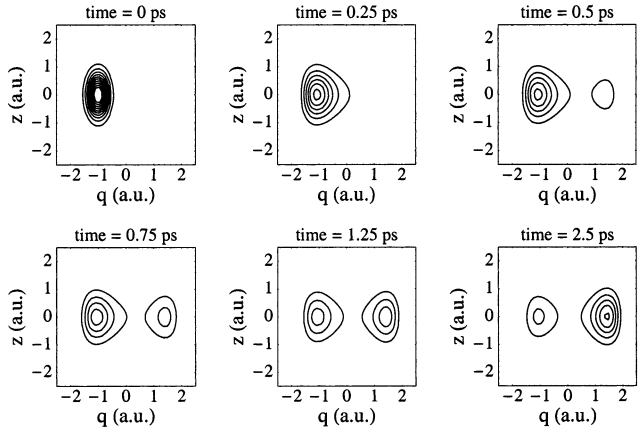

Figure 5. Time-evolution of $\exp(g(q, z))$ at $T = 500$ K.

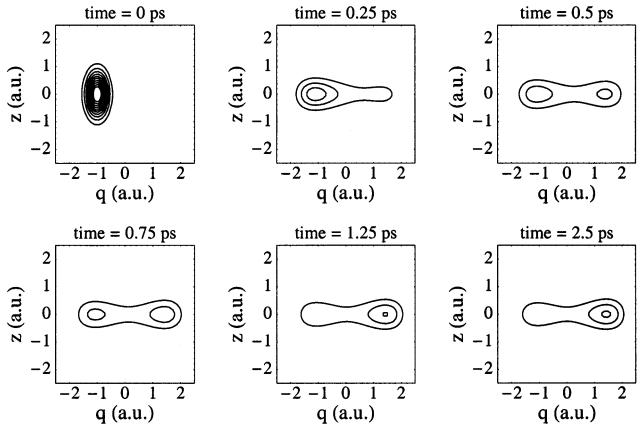

Figure 6. Time-evolution of $\exp(g(q, z))$ at $T = 1200$ K.

by

$$\rho_{eq} = \frac{\exp(-\hat{H}/kT)}{\mathrm{Tr}(\exp(-\hat{H}/kT))} \tag{54}$$

Provided that the system is sufficiently simple, it is trivial to diagonalize $\hat{H}$ and compute both $\hat{\rho}_{eq}$ and the equilibrium expectation value of any operator. The variance of momentum operator $\hat{\rho}$ is related to a length scale

$$\lambda_c = \sqrt{\frac{\hbar^2}{2\langle \hat{p}^2 \rangle_{eq}}} \tag{55}$$

that determines the coherence length for the equilibrium state. At high temperatures, the eigenstates comprising the density matrix are for the most part uncorrelated with one another and $\langle \hat{p}^2 \rangle_{eq}$ is related to the thermal energy kT. As $T \rightarrow \infty$, the equilibrium coherence length asymptotically approaches the thermal de Broglie wavelength, precisely as predicted in the CL model. At low temperatures, λ_c will be governed by uncertainty rather than the bath's kinetic energy and as $T \rightarrow 0$, we would expect the system to be found in the pure ground state where the coherence length is maximized. To illustrate this, consider the curves shown in Figure 7. The solid line corresponds to the temperature dependence of the thermal de Broglie wavelength for the particle. The dashed curve describes the equilibrium coherence length for a harmonic oscillator and is given by

$$\lambda_c^{HO} = \sqrt{\frac{\hbar}{2m\omega}\left(\langle n \rangle_{eq} + \frac{1}{2}\right)^{-1}} \tag{56}$$

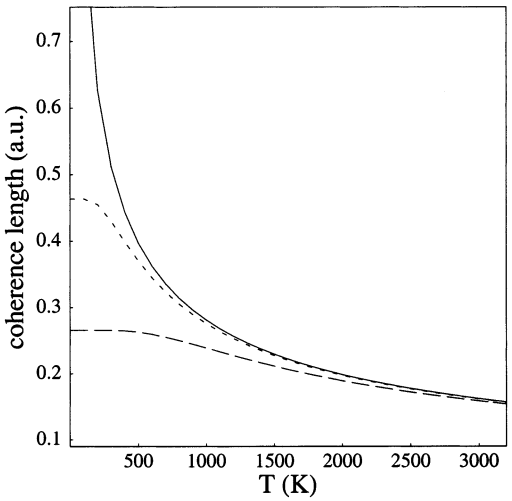

Figure 7. Coherence length as a function of bath temperature. At high temperatures the coherence length is equivalent to the thermal de Broglie wavelength (solid curve). At low temperatures the zero-point motion of the system becomes more important and the coherence length should roll-over as the temperature approaches zero as indicated in the dotted and dashed curves.

where

$$\langle n\rangle_{\mathrm{eq}} = \frac{1}{\exp(\hbar\omega/kT) - 1} \tag{57}$$

is the average number of quanta in the oscillator at thermal equilibrium. The dotted line is λ_c for a particle evolving on a potential surface depicted in Figure 4. The breakdown of the high-temperature limit is clearly evident. At low temperatures, the thermal de Broglie wavelength is much larger than the coherence length for the pure ground state. According to eq 28 the decoherence time scale will be very long, resulting in the buildup of coherences between position eigenstates for which there is no appreciable population. This problem is resolved in the dotted and dashed curves where the coherence length and decoherence time scale are finite for all temperatures. Figure 7 indicates that a low temperature the equilibrium coherence length is equivalent to the thermal de Broglie wavelength at a higher temperature thus from the viewpoint of the CL model, the contribution of the zero-point energy to the equilibrium coherence length is tantamount to an effective temperature. We can use eqs 54 and 55 to compute a back-of-the-envelope coherence length to replace the thermal de Broglie wavelength in eq 44 and thereby approximate the low-temperature dynamics of an arbitrary potential well.

Finally, we consider a classical ensemble of 500 particles, where the initial phase space distribution is determined by the Wigner function for the initial state of the previous cases. The classical particles evolve according to the Langevin equation given by eq 22. We determine the stochastic forces $F(\delta t)$ acting on the particles by choosing a set of psuedorandom numbers from a Gaussian probability distribution

$$P[F(\delta t)] = \sqrt{\frac{\delta t}{8\pi m\gamma kT}}\exp\left(-\frac{q^2\delta t}{4m\gamma kT}\right) \tag{58}$$

where γ^{-1} is the relaxation rate, kT is the thermal energy of the bath, and δt is the time scale over which the random forces act.[48] The particles are then propagated according to the standard Verlet algorithm for solving Newton's equations.

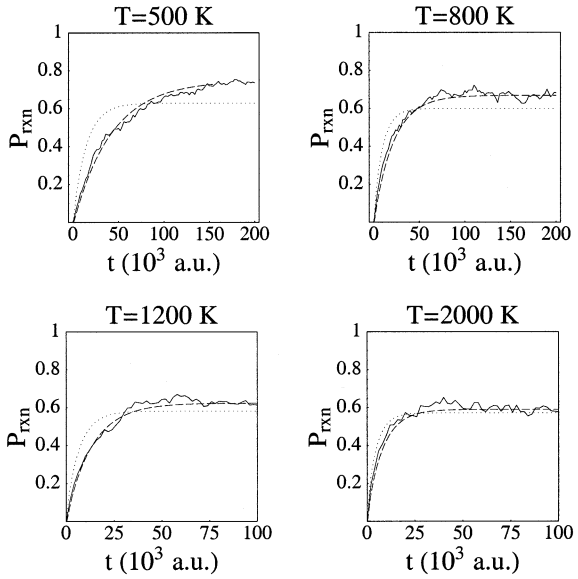

Figure 8. P_{rxn} as a function of time and temperature. The solid curves correspond with a classical Langevin simulation involving 500 particles. The dashed curves represent the semiclassical calculation where the coherence length is given by the thermal de Broglie wavelength Λ. The dotted curves are associated with the semiclassical calculation using the equilibrium coherence length λ_c.

For the two semiclassical systems the reaction probability at a given instant in time is given by the integral

$$P_{\mathrm{rxn}} = \int_0^\infty \exp(g^{(0)}(q))\,\mathrm{d}q \tag{59}$$

where the transition state at $q = 0$ defines the dividing surface separating the reactants and products. In the classical simulation we simply count the number of particles on the product side of this surface and divide by the total number of particles in the ensemble

$$P_{\mathrm{rxn}} = \frac{N_{q>0}}{N_{\mathrm{total}}} \tag{60}$$

Figure 8 shows P_{rxn} as a function of both time and temperature for the three cases. Because the reaction is energetically downhill, the overall reaction probability decreases with increasing temperature due to the fact that back-reaction is more likely to occur at larger thermal energies. As the temperature decreases, the dotted curve begins to deviate from the dashed and solid curves. This illustrates the significance of the coherence length scale in our calculations. At high temperatures $\lambda_c \rightarrow \Lambda$; hence there is only a slight difference between the classical and semiclassical curves at $T = 2000$ K. For lower temperatures, however, the λ_c is dominated by quantum fluctuations associated with zero-point motion rather than thermal fluctuations and the difference between the semiclassical calculations becomes more apparent. Eventually, the kinetic energy fluctuations in the quantum state become greater than the thermal fluctuations predicted by the Caldeira−Leggett model and the high-temperature approximation breaks down.

VI. Conclusions

In this paper we have constructed a novel hydrodynamic method for propagating the quantum density matrix based upon its moments and momentum cumulants. This procedure offers certain advantages over the usual Bohmian formulation, in that the basic equations of motion involve only first-order derivatives

of the cumulants. The price we pay for this simplification is that we have an infinite hierarchy of moments equations. However, in the presence of a dissipative bath, the cumulants are damped and we can obtain approximate closure at an arbitrarily high order. In the limit of high temperatures where decoherence is exceedingly rapid, we have found success in truncating the dynamics at second-order in the cumulants. Our approach allows us to incorporate the ideas of quantum nonlocality and kinetic-energy fluctuations into the equations of motion. However, the resulting equations are more or less classical since they can be derived from a moment expansion of the density matrix. This suggests a systematic way of introducing quantum effects such as dynamical tunneling and zero-point motion into multidimensional classical MD or Monte Carlo simulations. The method we foresee involves a cellular discretization of phase space wherein the moments of the classical probability distribution provide an auxiliary ensemble force that supplements the classical force in driving a swarm of trajectories.

Acknowledgment. We acknowledge Dr. I. Burghardt for discussions. This work was funded by the National Science Foundation (CAREER award) and the R. A. Welch Foundation.

References and Notes

(1) Allen, M. P.; Tildesley, D. J. *Computer Simulation of Liquids*; Oxford University Press: Oxford, U.K., 1987.
(2) Rapaport, D. C. *The Art of Molecular Dynamics Simulation*; Cambridge University Press: Cambridge, U.K., 1995.
(3) Dey, B. K.; Askar, A.; Rabitz, H. *J. Phys. Chem.* **1998**, *109*, 8770.
(4) Lopreore, C. L.; Wyatt, R. E. *Phys. Rev. Lett.* **1999**, *82*, 5190.
(5) Burant, J. C.; Tully, J. C. *J. Chem. Phys.* **2000**, *112*, 6097.
(6) Bittner, E. R. *J. Chem. Phys.* **2000**, *112*, 9703.
(7) Martens, C. C.; Fang, J. *J. Chem. Phys.* **1997**, *106*, 4918.
(8) Donoso, A.; Martens, C. C. *J. Chem. Phys.* **2000**, *112*, 3980.
(9) Donoso, A.; Kohen, D.; Martens, C. C. *J. Chem. Phys.* **2000**, *112*, 7345.
(10) D., A. D.; Martens, C. C. *Phys. Rev. Lett.* **2001**, *87*, 223202.
(11) Miller, W. H. *J. Phys. Chem. A* **2001**, *105*, 2942.
(12) Billing, G. D. *Chem. Phys. Lett.* **2001**, *339*, 237.
(13) Billing, G. D. *Chem. Phys.* **2001**, *264*, 71.
(14) Billing, G. D. *Int. J. Quantum Chem.* **2001**, *00*, 1.
(15) Billing, G. D. *J. Phys. Chem. A* **2001**, *105*, 2340.
(16) de Broglie, L. *C. R. Acad. Sci. Paris* **1927**, *184*, 273.
(17) Bohm, D. *Phys. Rev.* **1952**, *85*, 166.
(18) Bohm, D. *Phys. Rev.* **1952**, *85*, 180.
(19) Holland, P. R. *The Quantum Theory of Motion*; Cambridge University Press: Cambridge, U.K., 1993.
(20) Liszka, T. J.; Duarte, C. A. M.; Tworzydlo, W. W. *Comput. Methods Appl. Mech. Eng.* **1996**, *139*, 263.
(21) Wyatt, R. E. *J. Chem. Phys.* **1999**, *111*, 4406.
(22) Lopreore, C. L.; Wyatt, R. E. *J. Chem. Phys.* **2002**, *116*, 1228.
(23) Bittner, E. R.; Wyatt, R. E. *J. Chem. Phys.* **2000**, *113*, 8898.
(24) Wyatt, R. E.; Bittner, E. R. *J. Chem. Phys.* **2000**, *113*, 8888.
(25) Mayor, F. S.; Askar, A.; Rabitz, H. *J. Phys. Chem.* **1999**, *111*, 2423.
(26) Wyatt, R. E.; Lopreore, C. L.; Parlant, G. *J. Chem. Phys.* **2001**, *114*, 5113.
(27) Na, Y.; Wyatt, R. E. *Phys. Rev. E* **2001**, *65*, 016702.
(28) Maddox, J. B.; Bittner, E. R. *J. Chem. Phys.* **2001**, *115*, 6309.
(29) Maddox, J. B.; Bittner, E. R. *Phys. Rev. E* **2002**, *65*, 026143.
(30) Burghardt, I.; Cederbaum, L. S. *J. Chem. Phys.* **2001**, *115*, 10303.
(31) Burghardt, I.; Cederbaum, L. S. *J. Chem. Phys.* **2001**, *115*, 10312.
(32) Ploszajczak, M.; Rhoades-Brown, M. J. *Phys. Rev. Lett.* **1985**, *55*, 147.
(33) Lill, J. V.; Haftel, M. I.; Herling, G. H. *J. Chem. Phys.* **1989**, *90*, 4940.
(34) Lill, J. V.; Haftel, M. I.; Herling, G. H. *Phys. Rev. A* **1989**, *39*, 5832.
(35) Johansen, L. M. *Phys. Rev. Lett.* **1998**, *80*, 5461.
(36) Wigner, E. P. *Phys. Rev.* **1932**, *40*, 749.
(37) McQuarrie, D. A. *Statistical Mechanics*; Harper and Row: New York, 1976.
(38) Kohen, D.; Marston, C. C.; Tannor, D. J. *J. Chem. Phys.* **1997**, *107*, 5236.
(39) Feynman, R. P.; Vernon, F. L. *Ann. Phys. (N. Y.)* **1963**, *24*, 118.
(40) Calderia, A. O.; Leggett, A. J. *Physica* **1983**, *121A*, 587.
(41) Unruh, W. G.; Zurek, W. H. *Phys. Rev. D* **1989**, *40*, 1071.
(42) Hu, B. L.; Paz, J. P.; Zhang, Y. *Phys. Rev. D* **1992**, *45*, 2843.
(43) Hu, B. L.; Paz, J. P.; Zhang, Y. *Phys. Rev. D* **1993**, *47*, 1576.
(44) Zwillinger, D. *Handbook of Differential Equations*; Academic Press: 1989.
(45) Maddox, J. B.; Bittner, E. R.; Burghardt, I. *Int. J. Quantum Chem.* **in press**,.
(46) Lee, H. W. *Phys. Rep.* **1995**, *259*, 147.
(47) Light, J. C.; Hamilton, I. P.; Lill, J. V. *J. Chem. Phys.* **1982**, *82*, 1400.
(48) Thijssen, J. M. *Computational Physics*; Cambridge University Press: 1995.